ARTICLE

# Effect of Hydrogen Addition on Methane HCCI Engine Ignition Timing and Emissions Using a Multi-zone Model

Zi-han Wang[a], Chun-mei Wang[a]*, Hua-xin Tang[a], Cheng-ji Zuo[a], Hong-ming Xu[b]

*a. School of Mechanical and Automotive Engineering, Hefei University of Technology, Hefei 230009, China*

*b. Mechanical and Manufacturing Engineering, School of Engineering, The University of Birmingham, Edgbaston, Birmingham B15 2TT, UK*

(Dated: Received on November 4, 2008; Accepted on January 19, 2009)

Ignition timing control is of great importance in homogeneous charge compression ignition engines. The effect of hydrogen addition on methane combustion was investigated using a CHEMKIN multi-zone model. Results show that hydrogen addition advances ignition timing and enhances peak pressure and temperature. A brief analysis of chemical kinetics of methane blending hydrogen is also performed in order to investigate the scope of its application, and the analysis suggests that OH radical plays an important role in the oxidation. Hydrogen addition increases $NO_x$ while decreasing HC and CO emissions. Exhaust gas recirculation (EGR) also advances ignition timing; however, its effects on emissions are generally the opposite. By adjusting the hydrogen addition and EGR rate, the ignition timing can be regulated with a low emission level. Investigation into zones suggests that $NO_x$ is mostly formed in core zones while HC and CO mostly originate in the crevice and the quench layer.

**Key words:** Homogeneous charge compression ignition, Multi-zone model, Methane, Hydrogen, Ignition timing, Emission

## I. INTRODUCTION

Homogeneous charge compression ignition (HCCI) is attracting more and more attention for it combines advantages of conventional compression ignition (CI) and spark ignition (SI). It has high thermal efficiency, fuel economy and the potential in reducing particulate matter (PM) emission as it has a higher air/fuel ratio. Because of its low-temperature combustion, it reduces nitrogen oxides ($NO_x$) emission. Furthermore, HCCI has proved to be fuel flexible, since it has been achieved with traditional liquid fuels like gasoline or diesel as well as gaseous fuel such as propane or natural gas. It meets the demand for cleaner emissions, high efficiency and reducing the tension on the limited supply of fossil fuels. HCCI has been successfully applied to both gasoline and diesel engines. All the virtues above render it the possibility of replacing traditional engines [1-5].

The difficulty in applying the HCCI engine to practical use lies partly in the fact that it is hard to control its ignition timing, burning rate, and cold-start capability (especially for HCCI engine with a low compression ratio or with high octane rating fuel) [6]. The expansion of operating region is another issue. Among them, controlling the ignition timing and burning rate should get special attention since they are connected with emissions and power output. Using variable valve timing to change exhaust gas recirculation (EGR) rate was considered as a solution to control the ignition timing [7-13]. By varying the amount of hot residual burned gases (internal EGR) the in-cylinder pressure and temperature will change, and the ignition property can be adjusted. Although this technique is particularly attractive and its time response could be made sufficiently fast to handle rapid transients, it requires a specially designed valvetrain. An alternative solution is to use a mixture of two fuels. Adjusting the proportion of two fuels with different ignition properties has been reported as an effective technique to control the ignition timing and load in HCCI combustion [14-19].

Natural gas (mainly methane) is used as fuel increasingly due to its large supply and relatively large heat release output and extended lean operational mixture region. However, the auto-ignition of natural gas under diesel-like conditions needs a temperature as high as 1200-1250 K [20]. Such a high temperature requires either high compression ratio or high intake air temperature. Both of the requirements have negative effects on engine performance and durability. One solution is to add hydrogen to natural gas [21]. The hydrogen can be conveniently obtained through exhaust gas fuel reforming at low temperatures [22].

Hydrogen has a much faster burning rate, good lean

*Author to whom correspondence should be addressed. E-mail: chunmei.wang@hotmail.com, Tel.:+86-551-2901756-2606

 

burn property and high heat release output. The use of hydrogen as an additive can affect the onset of HCCI combustion by altering the main heat release delay and acting as an ignition improver. It enables a natural gas engine to operate at leaner conditions. Such a lean operation can improve power production efficiency, help maintain the combustion stability, and lower emissions, especially those of HC and CO. Much work has been done in this area. For example, Philippe obtained a detailed kinetic scheme for hydrogen blending methane combustion [15].

The present numerical simulation is intended to investigate and quantify the effect of hydrogen addition on the combustion characteristics and emissions of methane HCCI engine, and find a strategy to optimize the combustion mode. The ignition timing and the chemical kinetics are studied, and the emissions of $NO_x$, HC and CO are predicted. The results are compared with that derived from a single-zone model to testify to the multi-zone model's superiority. A parametric study was carried out to quantify the effects of EGR on ignition timing and emissions. The ignition timing can be regulated in a suitable range with low emissions by adjusting the relative proportion of hydrogen addition and EGR rate.

## II. MODEL AND INITIAL CONDITIONS

Chemical kinetics plays an important part in HCCI auto-ignition characteristics. The CHEMKIN package was used in this work because it facilitates the formation, solution, and interpretation of problems involving elementary gas-phase chemical kinetics, which is quite favorable for the analysis of gaseous fuel combustion.

Two models are used for the simulation. The single-zone model treats the whole combustion chamber as a single zone and the spatial heterogeneity of gas temperature and composition is eliminated. Simulation results from the single-zone model usually show unrealistic sharp pressure and temperature increase, and short burn duration. Unlike the single-zone model, the multi-zone model divides the chamber into a finite number of zones with different initial temperatures and compositions, analogous to the heterogeneity within the cylinder of real engines (*e.g.* different temperature, compositions and local EGR rates in the crevice volume, the thin quench layer, and central core zones). Each zone is assumed to have constant mass. The interactions between zones can only be realized by volume work. The multi-zone model has been employed by many researches as it represents more realistic situation in the cylinder [23-31]. For example, Easley *et al.* divided the chamber into four typical zones (*i.e.* core zone, outer core zone, quench layer, and crevice) and studied the emission of $NO_x$, HC, and CO [23].

By coupling the first law of thermodynamics ($Q-W=\Delta U$) and the state equation of ideal gas ($pV=nRT$), the governing equation for each zone in the multi-zone model can be written as:

$$\begin{aligned}\overline{c}_{p,i}\frac{\mathrm{d}T_i}{\mathrm{d}t} &= -\frac{1}{\rho}\sum_{j=1}^{k} u_j\,\dot{\omega}_j\,M_j - \frac{\dot{Q}_{hli}}{m_i} - \\ &\quad \overline{R}_i T_i\left[\frac{1}{V}\frac{\mathrm{d}V}{\mathrm{d}t} - \frac{\sum_{i=1}^{n} m_i\overline{R}_i\frac{\mathrm{d}T_i}{\mathrm{d}t}}{\sum_{i=1}^{n} m_i\overline{R}_i T_i}\right] \qquad (1)\end{aligned}$$

where $i$ and $j$ are the indexes of zones and chemical species, $n$ and $K$ represent total number of zones and species, $\overline{c}_p$ and $\overline{R}$ are average specific heat (at constant pressure) and average gas constant for each zone, $T$, $\rho$, $m$, and $\dot{Q}_{hl}$ are temperature, density, mass and rate of heat loss for each zone, $u$, $\omega$, and $M$ are internal energy, molar production rate, and molecular weight for each zone, $V$ is the total cylinder volume (plus user-defined crevice volume), and $t$ is the time.

The mass fraction of species $j$, $Y_j$, for each zone is calculated at each time increment from a set of ordinary differential equations (ODEs)

$$\begin{aligned}\frac{\mathrm{d}Y_j}{\mathrm{d}t} &= \frac{\dot{\omega}_j M_j}{\rho_i} \\ &(i = 1,\ldots,n \text{ and } j = 1,\ldots,K) \qquad (2)\end{aligned}$$

CHEMKIN subroutines are called to calculate the values on the right-hand side of each ODE in Eq.(2).

In order to directly calculate the temperature derivative ($\mathrm{d}T_i/\mathrm{d}t$) of each zone in Eq.(2), it needs to be written in the form of Eq.(3), such that the temperature derivative for each zone is independent of the temperature derivative for other zones.

$$\begin{aligned}A_{mm}\frac{\mathrm{d}T_n}{\mathrm{d}t} &= B_m \\ &(m = 1,\ldots,N \text{ and } n = 1,\ldots,N) \qquad (3)\end{aligned}$$

Once the set of $n$ ODEs in Eq.(3) is defined in the user-written main programs, CHEMKIN subroutines are called to calculate the coefficients of the equation set ($A_{mm}$ and $B_m$). A Gaussian elimination subroutine is then called to explicitly define the temperature derivative of each zone, *i.e.* to calculate the value of $f$ on the right-hand side of each ODE in Eq.(4).

$$\frac{\mathrm{d}T_i}{\mathrm{d}t} = f \quad (i = 1,\ldots,n) \qquad (4)$$

The final set of ODEs to be solved consists of Eqs.(2) and (4), containing in total ($n$+$K$) ODEs ($n$ ODEs for the temperature derivative of each of the $n$ zones in Eq.(5) and $K$ ODEs for $K$ chemical species in each zone in Eq.(2)). The code then solves for these variables (temperature $T$ for each zone and mass fraction $Y$ for each species) sequentially (zone by zone) from zone 1 to

DOI:10.1088/1674-0068/22/03/290-296 

zone $n$, using a FORTRAN ODE solver DVODE, for a user-defined time span. After zonal temperature $T_i$ is calculated by DVODE, the cylinder pressure (assumed uniform across all zones) can be derived from Eq.(5):

$$p = \frac{1}{V}\sum_{i=1}^{n} m_i \overline{R}_i T_i \tag{5}$$

Mass exchange among zones is not considered here. Heat transfer between the chamber and cylinder wall is considered using heat transfer equation

$$Q = h_{\rm c} A(T - T_{\rm w}) \tag{6}$$

where $T$ is the average temperature inside the cylinder, $T_{\rm w}$ is the temperature at cylinder wall, $A$ is the surface area, and $h_{\rm c}$ is heat transfer coefficient which can be acquired from Woschni equation [32].

Theoretically, results will draw closer to the real situation with the increase of the numbers of zones. However, computing time also increases. Comparing 10-zone model with 20- and 40-zone model, it has been shown that zone numbers only slightly affect HC and $NO_x$ emission results, although they have a greater influence on CO emission [27]. In this work, the entire engine is divided to 9 zones. The crevice, the area above and surrounding the first piston ring, which is crucial for the formation of HC and CO, is defined as zone 1. The quench layer, the outmost zone in the chamber, is defined as zone 2. Zone 3 is at the inner side of zone 2. Zones 3-9 gradually approach the core in the chamber. Zone 9 is the core in the chamber.

For the multi-zone CHEMKIN model, the user needs to define the following parameters: (i) fuel composition in mole fraction; (ii) intake valve close (IVC) and exhaust valve open (EVO) in crank angle; (iii) initial in-cylinder pressure at IVC; (iv) engine geometry (bore, stroke, connecting rod length, compression ratio); (v) cylinder wall temperature and Woschni heat transfer scaling factor; (vi) number of zones; (vii) for each zone, the equivalence ratio, residual mass fraction, temperature, and mass percentage of the total mass within the cylinder.

A correct assumption of the initial conditions at IVC is crucial for a match of simulation results and experimental data. The most reliable way is to use the information provided from the experimental data if it is available. If not all the information is available from test data, some simulation has to be done in advance. In this work, initial conditions are obtained from Ref.[33]. The specifications of four valves per cylinder, as initial condition, are bore of 81.6 mm, stroke of 88.2 mm, compression ratio of 15.0, pressure at IVC of $10^5$ Pa, and revolutions per minute (RPM) of 1500.

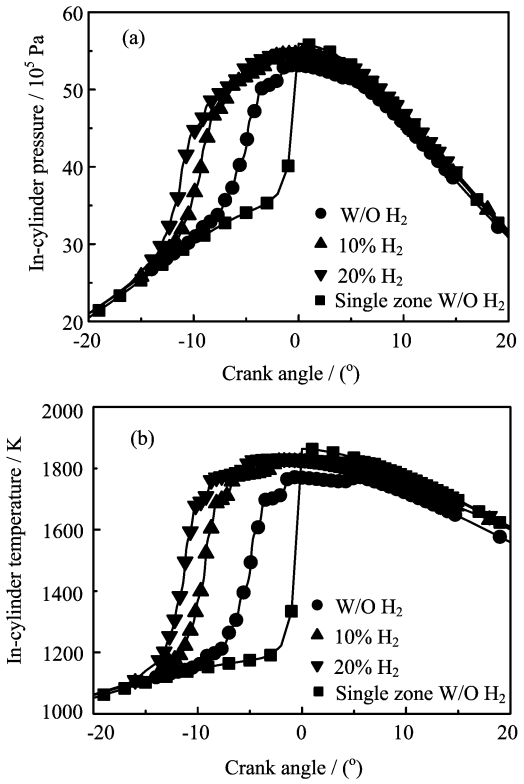


FIG. 1 Effect of $H_2$ on in-cylinder temperature and pressure with multi-zone model.

## III. RESULTS AND DISCUSSION

### A. Effect on ignition timing

Figure 1 shows the pressure and temperature with the molar fraction of hydrogen varying between 0 and 20% and the same other parameters. It shows clearly the advance of auto-ignition timing due to $H_2$ addition. About 8 CAD of ignition timing advance is achieved with 20% of $H_2$ addition. From no hydrogen to 10% of hydrogen addition, the ignition timing is advanced by approximately 5 CAD. Upon reaching 10% and continuously increasing hydrogen, the benefit appears to be less significant. For $H_2$ addition from 10% to 20%, the ignition timing advances by 3 CAD. A higher temperature and pressure is achieved with the increase of $H_2$ due to the fact that $H_2$ has a higher heat release. The pressure and temperature from single-zone model are also plotted; they exhibit sharp increases when ignition starts and an abrupt turn near the top dead center (TDC) which may not be realistic.

In Fig.2, mass fraction burnt (MFB), which indicates combustion development, is compared with that from experiment. It shows that the simulation results agree well with the experimental results. Heat release rate is shown in Fig.3. It can be seen that $H_2$ addition leads to an advance in heat release and an increase in the peak of heat release rate. The kinks in these traces are due

DOI:10.1088/1674-0068/22/03/290-296 

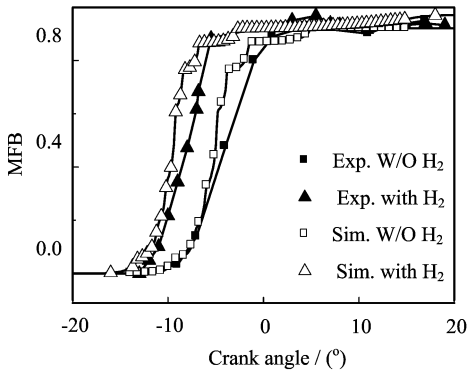


FIG. 2 Mass fraction burned (MFB) for 0 and 10% of $H_2$ addition (simulation and experimental results comparison).

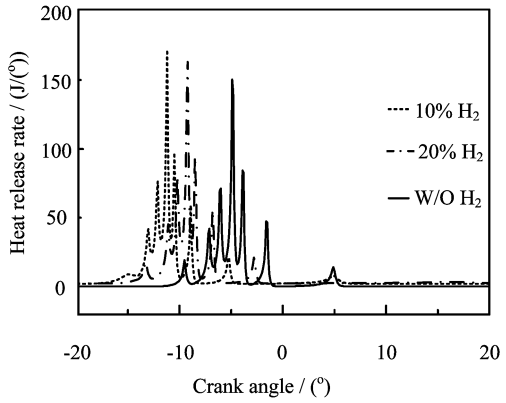


FIG. 3 Effect of $H_2$ on heat release rate.

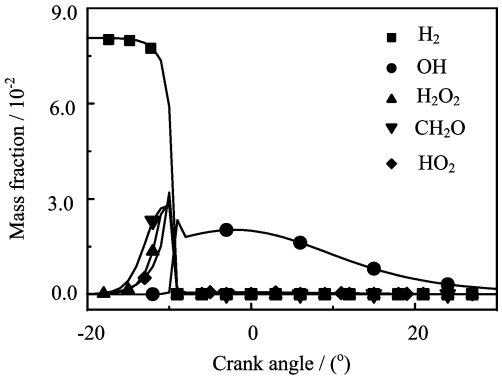


FIG. 4 Crucial radicals during oxidation with 20% of $H_2$ addition.

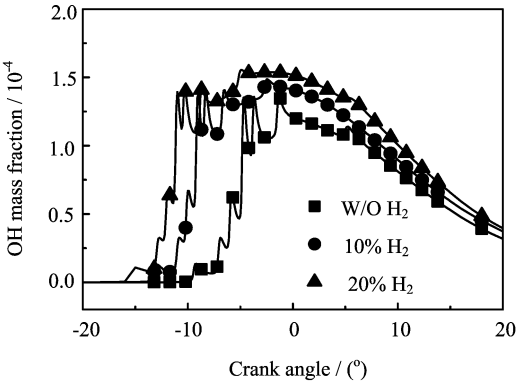


FIG. 5 Effect of $H_2$ on radical OH.

to the heterogeneity in temperature and compositions among zones and they can be avoided by using single-zone model. Figure 4 shows $H_2$, $H_2O_2$, OH, $CH_2O$ and $HO_2$ radicals for 20% of $H_2$ addition and 20% of EGR rate. These substances are crucial for $CH_4$ oxidation. It can be seen that at 20 CAD before TDC (bTDC), the amount of $H_2$ decreases rapidly while the amounts of $CH_2O$, $HO_2$, and $H_2O_2$ increase sharply, making preparation for the formation of OH. At about 10 CAD bTDC, radicals $CH_2O$, $HO_2$, and $H_2O_2$ react with $H_2$ quickly to produce OH, and the amount of OH increases quickly. At 3 CAD bTDC, $CH_4$ oxidation dominates, and OH is consumed rapidly. The important reactions are listed below [15]:

$$\begin{aligned}
H_2 + OH &= H_2O + H && (7)\\
H + O_2 + M &= HO_2 + M && (8)\\
CH_4 + H &= CH_3 + H_2 && (9)\\
HO_2 + HO_2 &= H_2O_2 + O_2 && (10)\\
CH_3 + HO_2 &= CH_3O + OH && (11)\\
H + HO_2 &= OH + OH && (12)\\
H_2O_2 + M &= OH + OH + M && (13)\\
OH + CH_4 &= CH_3 + H_2O && (14)
\end{aligned}$$

Brief analysis of the chemical kinetics will provide a better understanding of the combustion process. $H_2$ addition leads to an increase in radical H according to reaction (7). H contributes to the production of $HO_2$ and $CH_3$ via reactions (8) and (9) respectively. $HO_2$ partially converts to $H_2O_2$ via reaction (10). $CH_3$, $HO_2$ and $H_2O_2$ are crucial radicals and they promote the formation of OH via reactions (11), (12), and (13). OH plays a crucial role in the oxidation of $CH_4$ via reaction (14). Thus $H_2$ addition leads to more OH radicals, the ignition is advanced, and the temperature and the pressure are enhanced. This can be seen from Fig.5.

When the air, fuel, and hot EGR are mixed, the initial temperature of the mixture at IVC can be estimated from Eq.(15) [13]:

$$T_{\rm total} = T_{\rm air/fuel}(1 - y_{\rm ERG}) + T_{\rm EGR} y_{\rm EGR} \qquad (15)$$

where $y_{\rm EGR}$ is the molar fraction of the mixture and can be defined as:

$$y_{\rm EGR} = \frac{n_{\rm EGR}}{n_{\rm air/fuel} + n_{\rm EGR}} \qquad (16)$$

here, $n_{\rm EGR}$ and $n_{\rm air/fuel}$ are the molar of EGR and air/fuel mixture respectively.

DOI:10.1088/1674-0068/22/03/290-296 

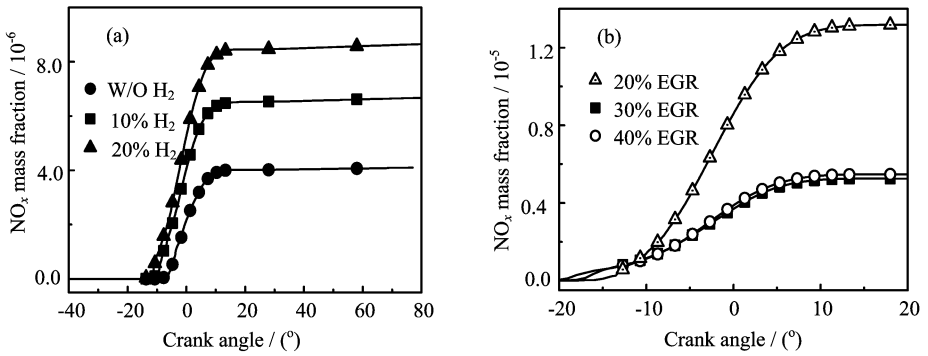


FIG. 6 Effect of $H_2$ and EGR rate on $NO_x$ emission.

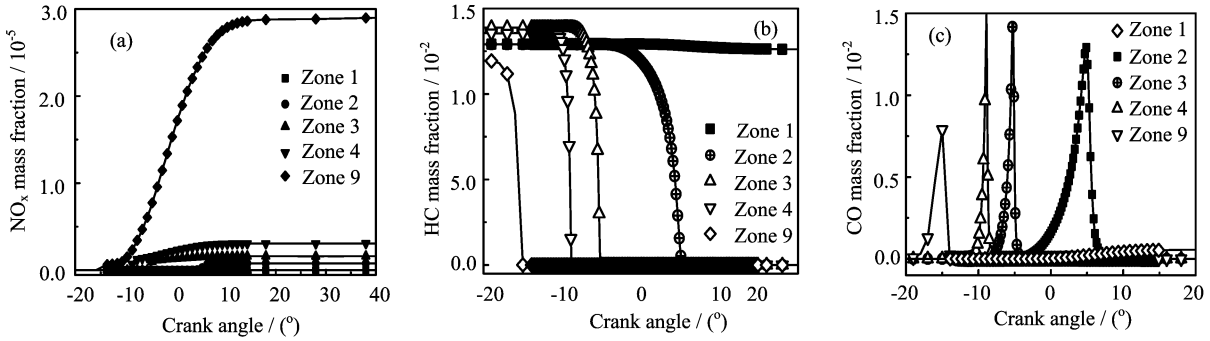


FIG. 7 $NO_x$ (a), HC (b), and CO (c) emission in zones 1, 2, 3, 4, and 9 for 20% of $H_2$ addition.

### B. Effect on emissions

#### 1. Effect on $NO_x$

The HCCI engine greatly reduces the emission of $NO_x$ because HCCI combustion does not have high temperature regions and high concentration regions which are crucial for $NO_x$ formation. $NO_x$ formation is primarily dominated by the temperature. There is almost no $NO_x$ formation for temperatures below 1800 K, while $NO_x$ formation progressively speeds up when the temperature exceeds 2000 K.

Figure 6(a) shows that the $H_2$ addition increases the emission of $NO_x$ due to an increase in the temperature. When the amount of $H_2$ increases from 0 to 10%, $NO_x$ is nearly doubled. However, for $H_2$ addition from 10% to 20%, $NO_x$ increases by only about 15%, so this trend is less significant. The peak temperature for each case is below 2000 K. The overall $NO_x$ emission is low, and the mass fraction of $NO_x$ is lower than $10^{-5}$.

The effects of EGR rate on the $NO_x$ emission are shown in Fig.6(b) ($H_2$ addition is fixed at 20%). An increase in EGR rate significantly inhibits $NO_x$ formation, For EGR from 20% to 30%, $NO_x$ is reduced by about 80%. In contrast, there are no big differences in $NO_x$ emissions for EGR rate from 30% to 40% due to a comparable peak temperature in the two cases.

The $NO_x$ for 20% of $H_2$ addition and 20% of EGR in zones 1-4 and zone 9 is shown in Fig.7. The inner core zone–zone 9, is the major source of the $NO_x$ emission. The figure shows that $NO_x$ in zone 9 is almost seven times the average $NO_x$ in zones 1-4. The peak temperature of outer core zones is relatively low, and the $NO_x$ emission is rather low there. The temperature of outer core zones, zones 3 and 4, gradually rises when heat generated in inner core zones is transferred there and the reaction is able to start. The quench layer (zone 2) and the crevice (zone 1), where the temperature is influenced by the cold cylinder wall, almost have no $NO_x$.

#### 2. Effect on HC

Unburned HC is usually formed in the quench layer and the crevice in traditional engines where the temperature is not high enough to oxidize fuel completely. It can be seen from Fig.8(a) that with the increase of $H_2$ addition, HC decreases and the oxidation advances.

The emission of HC in zones 1-4 and zone 9 is shown in Fig.7. The HC emission in each zone before oxidization is almost constant and has little difference. Zone 2 has a delay in oxidation because the temperature at quench layer is not high enough to oxidize the fuel. It has to wait for the heat transferred from the inner core zones to trigger HC oxidization. Zone 1 (crevice)

DOI:10.1088/1674-0068/22/03/290-296 

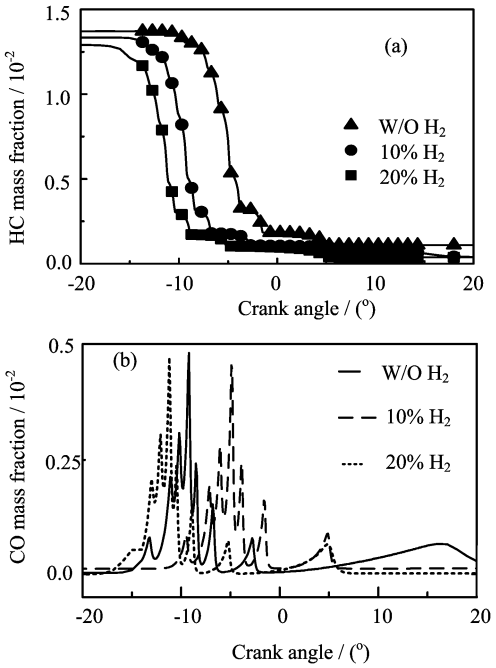


FIG. 8 Effect of $H_2$ on HC (a) and CO (b) emission.

has a longer delay in oxidation before reaction due to a low temperature, and the reaction cannot progress completely there. Only a small fraction of HC is oxidized and the rest remains as residual gas.

### 3. Effect on CO

CO is one of the intermediate products of combustion and is controlled by chemical kinetics. It is considered to be formed in the crevice and the quench layer where the temperature is not high enough to oxidize HC completely and prevents CO from oxidizing to $CO_2$. For this mechanism, wall temperature has strong impact on the CO emission.

$H_2$ addition contributes to the decrease of CO emission in two ways: the hydrogen addition leads to a higher temperature which means a better oxidation; for a fixed mole of the fuel in the cylinder, the concentration of $CH_4$ decreases with the introduction of the hydrogen fuel, so CO is less likely to be produced. Figure 8(b) shows the CO emission for 0, 10% and 20% molar fraction of $H_2$ addition. When the same molar fraction of $CH_4$ is replaced by $H_2$, the total mass decreases. Thus, although the mass of CO reduces, its mass fraction is likely to increase. Figure 8(b) shows that the mass fraction of CO is the most at 10% of $H_2$ addition and the least at no $H_2$ addition.

Figure 7 shows the CO trace in zones 1-4 and zone 9. CO in zone 9 reacts earlier and has smaller peak mass fraction. As for the reactions from zone 4 to zone 2, each has a couple of crank angles delay from its inner neighbor zone, and the intermediate CO there is all consumed shortly after its formation. In zone 1 (crevice) where temperature is not high enough, oxidation is delayed and CO is not able to be consumed, so it remains at the same level until EVO due to the cooling of the cylinder wall.

## IV. CONCLUSION

Through the above simulations using CHEMKIN multi-zone model, the following conclusions are obtained: (i) $H_2$ is efficient in controlling (advancing) $CH_4$ combustion ignition timing because it has a faster burning rate. By adjusting the molar fraction of the two fuels, optimum combustion is able to be achieved. (ii) $H_2$ raises the peak pressure and temperature due to its high heat release output, and this facilitates $NO_x$ formation, and lower HC and CO formations. (iii) The single-zone model is not realistic because it shows a sharp increase in the pressure and temperature when ignition begins and an abrupt turn near the TDC. In comparison, the multi-zone model describes combustion in a more practical way. (iv) $NO_x$ is formed mainly in the inner core zones. HC and CO is mainly formed in zones with low temperature such as zone 1 (crevice) and zone 2 (quench layer).

## V. ACKNOWLEDGEMENT

This work was supported by the Natural Science Foundation of Anhui Province (No.090412030).

[1] T. Shudo, Society of Automotive Engineers 01, 0112 (2002).
[2] Z. Q. Zheng, M. F. Yao, Z. Chen, and B. Zhang, Society of Automotive Engineers 01, 2993 (2004).
[3] P. M. Najt and D. E. Foster, Society of Automotive Engineers 01, 0264 (1983).
[4] R. H. Tring, Society of Automotive Engineers 01, 2688 (1989).
[5] III T. W. Ryan and III A. W. Gray, Society of Automotive Engineers 01, 1676 (1997).
[6] M. F. Yao, Z. Chen, Z. Q. Zheng, B. Zhang, and Y. Xing, Fuel **85**, 2046 (2006).
[7] G. Kontarakis, N. Collings, and T. Ma, Society of Automotive Engineers. 01, 2870 (2000).
[8] L. Koopmans and I. Denbratt, Society of Automotive Engineers 01, 3610 (2001).
[9] D. Law, D. Kemp, J. Allen, Kirkpatrick G, and Copland T, Society of Automotive Engineers 01, 0251 (2000).
[10] L. Koopmans, R. Ogink, and I. Denbratt, Society of Automotive Engineers 01, 1854 (2003).
[11] J. O. Olsson, P. Tunestal, J. Ulfvik, and B. Johansson, Society of Automotive Engineers 01, 0743 (2003).

DOI:10.1088/1674-0068/22/03/290-296 

[12] Z. Peng, H. Zhao, and N. Ladommatos, Society of Automotive Engineers 01, 0747 (2003).
[13] R. Chen, N. Milovanovic, Int. J. Therm. Sci. **41**, 805 (2002).
[14] M. H. Morsy and S. H. Chung, Proc. IMechE. **221**, 605 (2007).
[15] D. Philippe and D. Guillume, Int. J. Hydrogen Energy **31**, 505 (2006).
[16] S. Toshio and Y. Hiroyuki, Int. J. Hydrogen Energy **32**, 2066 (2007).
[17] M. H. Morky, Fuel **86**, 533 (2007).
[18] S. C. Kong, Fuel **86**, 1483 (2007).
[19] A. Constantine, B. Choongsik, C. Roy, and K. Eiji, Fuel **87**, 1014 (2008).
[20] A. A. Agarwal and D. N. Assanis, Society of Automotive Engineers 01, 0136 (1998).
[21] Z. H. Huang, J. H. Wang, and B. Liu, Fuel **86**, 381 (2007).
[22] D. Yap, S. M. Peucheret, A. Megaritis, M. L. Wyszynski, and H. M. Xu, Fuel **31**, 587 (2006).
[23] W. L. Easley, A. A. Agarwal, and G. A. Lavoie, Society of Automotive Engineers 01, 1029 (2001).
[24] S. M. Aceves, D. L. Flowers, C. K. Westbrook, J. R. Smith, W. Pitz, R. Dibble, M. Christensen, and B. Johansson, Society of Automotive Engineers 01, 0327 (2000).
[25] S. M. Aceves, D. L. Flowers, J. Martinez-Frias, J. R. Smith, C. K. Westbrook, W. J. Pitz, R. Dibble, J. F. Wright, W. C. Akinyemi, and R. P Hessel, Society of Automotive Engineers 01, 1027 (2001).
[26] S. M. Aceves, J. Martinez-Frias, D. L. Flowers J. R. Smith, R. W. Dibble, J. F. Wright, and R. P. Hessel, Society of Automotive Engineers 01, 3612 (2001).
[27] D. L. Flowers, S. M. Aceves, J. Martinez-Frias, and R. W. Dibble, Proceedings of the Combustion Institute **29**, 687 (2002).
[28] S. M. Aceves, D. L. Flowers, F. Espinosa-Loza, J. Martinez-Frias, R. W. Dibble, M. Christensen, B. Johansson, and R. P. Hessel, Society of Automotive Engineers 01, 2869 (2002).
[29] S. M. Aceves, D. L. Flowers, F. Espinosa-Loza, J. Martinez-Frias, J. E. Dec, M. Sjoberg, R. W. Dibble, and R. P. Hessel, Society of Automotive Engineers 01, 1910 (2004).
[30] S. M. Aceves, D. L. Flowers, J. Martinez-Frias, F. Espinosa-Loza, M. Christensen, B. Johansson, and R. P. Hessel, Society of Automotive Engineers. 01, 2134 (2005).
[31] S. M. Aceves, D. L. Flowers, F. Espinosa-Loza, A. Babajimopoulos, and D. N. Assanis, Society of Automotive Engineers 01, 0115 (2005).
[32] J. B. Heywood, *Internal Combustion Engine Fundamentals*, New York: McGraw-Hill, 680 (1988).
[33] H. M. Xu, M. Liu, S. Gharahbaghi, and S. Richardson, Society of Automotive Engineers 01, 2123 (2005).

DOI:10.1088/1674-0068/22/03/290-296 